Available online at www.sciencedirect.com
SCIENCE DIRECT®
Solid State Sciences 8 (2006) 97–103
Solid State Sciences
www.elsevier.com/locate/ssscie

Dielectric and Raman spectroscopy of the heptaiodide complex $(\beta\text{-Cyclodextrin})_2\cdot CsI_7\cdot 13H_2O$

Vasileios G. Charalampopoulos [a], John C. Papaioannou [a,*], Haido S. Karayianni [b]

[a] Department of Chemistry, Laboratory of Physical Chemistry, National and Kapodistrian University of Athens, P.O. box 64004, 157 10 Zografou, Athens, Greece
[b] Laboratory of Physical Chemistry, Section of Materials Science and Engineering, School of Chemical Engineering, National Technical University of Athens, Iroon Polytechniou 9, Zografou 157 80, Athens, Greece

Received 18 July 2005; received in revised form 28 September 2005; accepted 22 October 2005

Available online 6 December 2005

Abstract

The frequency and temperature dependence of the real and imaginary parts of the dielectric constant (ε', ε''), the phase shift (ϕ) and the ac-conductivity (σ) of the polycrystalline $(\beta\text{-Cyclodextrin})_2\cdot CsI_7\cdot 13H_2O$ (β-Cs) have been investigated over the frequency and temperature ranges of 0–100 kHz and 140–425 K, respectively, in combination with Raman spectroscopy and DSC. The $\varepsilon'(T)$, $\varepsilon''(T)$ and $\phi(T)$ variations at frequency 300 Hz in the range 140 K $< T <$ 300 K show two sigmoids, two bell-shaped curves and two minima, respectively, revealing the existence of two kinds of water molecules, tightly bound and easily movable ones. β-Cs shows the transition of normal hydrogen bonds to those of flip-flop type at 199.9 K. As the temperature increases most of the thirteen water molecules per cyclodextrin dimer remain tightly bound and only a small number of them become easily movable. The DSC trace shows a small endothermic peak with an onset temperature of 80 °C, which is related to the easily movable water molecules. Strong peaks at 115 and 135 °C are caused by the tightly bound water molecules and the sublimation of iodine, respectively. The Cs^+ ions contribute to the ac-conductivity via a Grotthuss mechanism with an activation energy 0.64 eV when all the water molecules exist in the crystal lattice and 0.45 eV when the easily movable water molecules start to escape. The Raman peaks at 179, 170 and 166 cm^{-1} are due to the $I_2\cdot I^-{}_3\cdot I_2$ polyiodide chains consisting of $I^-{}_3$ units indicating charge transfer interactions and lengthening of I_2 units, respectively. The charge of $I^-{}_7$ units remains localized with negligible contribution to the conductivity until the sublimation of iodine starts.

Keywords: Dielectric properties; Raman spectra; β-Cyclodextrin complex; Heptaiodide ions; Flip-flop hydrogen bonds; Calorimetric measurement

1. Introduction

When β-Cyclodextrins (β-CDs) are crystallized from aqueous solutions with metal iodide/iodine, channel type complexes are formed in which the β-CD molecules are stacked like coins in a roll (head to head) and in their tubular cavity heptaiodide chains ($I_2\cdot I^-{}_3\cdot I_2$ in a Z-like form) are developed [1,2]. All of these systems have the same crystal structure (monoclinic $P2_1$) as $(\beta\text{-CD})_2\cdot KI_7\cdot 9H_2O$ which has been determined in detail by X-ray analysis [2]. This analysis showed that the atoms of I_2 units are disordered in positions with main occupancies I(4A) = 0.89, I(5A) = 0.70 and with minor occupancies I(4B) = 0.15, I(5B) = 0.14. Inversely, the iodine atoms I1, I2 of the central $I^-{}_3$ unit are in positions with full occupancy $(1, 0)$ (Fig. 1). X-ray, Far-Infrared and Raman study of polyiodide $(C_2H_5)_4N^+I^-{}_7$ complex by Nour, Chen and Laane [3], have also shown that $I^-{}_7$ ions are of type $I^-{}_3\cdot 2(I_2)$ with I_2 roughly perpendicular to the triiodide units.

The investigation of the dielectric relaxation properties of the β-CD complexes with Ba^{2+}, Cd^{2+} [4] and K^+, Li^+ [5,6] revealed the existence of two kinds of water molecules, tightly bound and easily movable ones. Specifically at temperatures $T <$ 330 K where all the water molecules exist in the lattice, the real part (ε') and imaginary part (ε'') of the dielectric constant as well as the phase shift (ϕ) showed two steps, two peaks and two minima, respectively. All systems also showed the transformation of normal hydrogen bonds to those of flip-flop type [7,8] at approximately 200 K. At temperatures $T >$ 330 K where the dehydration process starts the dielectric parameters ε', ε''

* Corresponding author.
E-mail address: jpapaio@cc.uoa.gr (J.C. Papaioannou).

1293-2558/$ – see front matter
doi:10.1016/j.solidstatesciences.2005.10.010

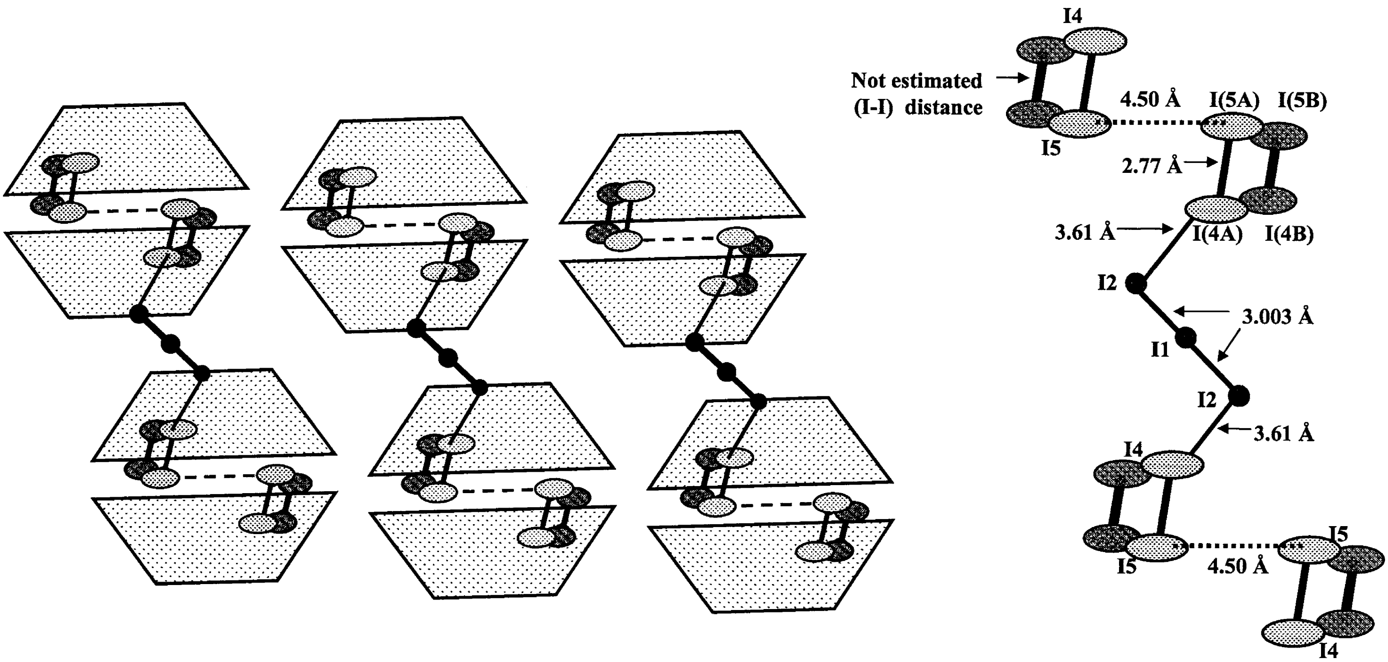

Fig. 1. Geometry of the dimers (two β-CD molecules head to head) and the polyiodide chain in the $(\beta\text{-CD})_2{\cdot}KI_7{\cdot}9H_2O$ complex according to Fig. 4 of Ref. [2].

are no longer sensitive to depict the polarization effects taking place because of the high conductivity values. The phase shift and the ac-conductivity however, could detect all the different processes in the samples.

The presence of two kinds of water molecules was also confirmed by the appearance of double endothermic peaks in the DSC traces which were directly related to the fractions of easily movable and tightly bound water molecules. These fractions depend on the progressive transformation

$$(H_2O)_{tightlybound} \rightarrow (H_2O)_{easilymovable}. \tag{1}$$

The contribution of the water-net work to the ac-conductivity (σ) of the above complexes is very important since it facilitates the relay mechanism of the proton transport. This process is amplified by the movements of metal ions which are fourfold coordinated by two water molecules and two hydroxyl groups in a near-tetrahedral arrangement [2]. As the temperature increases they become free to oscillate, contributing to the abrupt increase of the ac-conductivity (linear part in the $\ln\sigma$ vs $1/T$ plot) via a Grotthuss mechanism [9,10]. When the water molecules start to escape from the crystal-lattice the slope of the linear part decreases because of the gradual breakdown of the water-net work. This process renders the charges of the metal ions localized.

The contribution of the polyiodide chains to the ac-conductivity was determined by Raman spectroscopy. All of the above complexes showed an initial peak position of 179 cm^{-1} at 30 °C which shifted to 165–166 cm^{-1} at temperatures higher than 100 °C [4,6]. That happens because of the lengthening of the disordered I_2 units caused by a charge transfer interaction of $I^-{}_3$ units in each cyclodextrin dimer (order–disorder transition). The influence of the $I^-{}_7$ ions on the ac-conductivity is negligible until 130 °C approximately where the sublimation of iodine starts. This was confirmed by a third endothermic peak in the DSC traces and a rapid increase of the ac-conductivity in the $\ln\sigma$ vs $1/T$ plot.

Since the polyiodides present interesting electrical properties and many complicated structures [3,11], in the present work we investigate the dielectric properties of the $(\beta\text{-CD})_2{\cdot}CsI_7{\cdot}13H_2O$ complex (β-Cs) over the temperature region 140–425 K. Besides this, Raman spectra in combination with differential scanning calorimetry are recorded in the temperature region 300–425 K.

2. Experimental

β-Cyclodextrin, iodine and cesium iodide were purchased from Fluka. The preparation of the sample was carried out according to Ref. [1]. One gram of β-CD was dissolved in 80 ml of distilled water at room temperature under stirring until the solution became almost saturated. Then 0.59 g cesium iodide and 0.44 g solid iodine were added simultaneously to the solution and it was heated to 70 °C for 20–25 min. The hot solution was transferred quickly through a folded filter to an empty beaker (100 ml) which was covered with Teflon and then immersed in a Dewar flask (500 ml) containing water at the same temperature. After two days, very fine reddish-brown thin needles of β-Cs were grown with uniform composition. These were separated in a Buchner filter and dried in air. The water content of the crystals was determined by thermogravimetric analysis (NETZSCH-STA 409 EP, Controller TASC 414/3, heating rate 5 °C min^{-1}). The β-Cs complex was found to contain thirteen water molecules per dimer (Fig. 2), so the general composition is $(\beta\text{-CD})_2{\cdot}CsI_7{\cdot}13H_2O$. The number of water molecules was calculated from the weight loss in the temperature range of 25–125 °C, where all the wa-

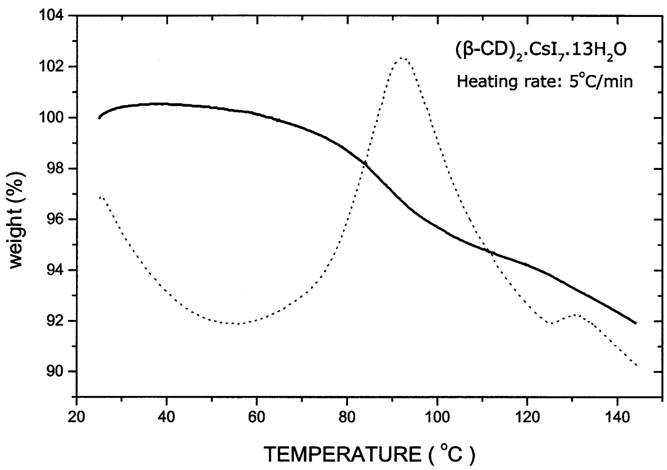

Fig. 2. Thermogravimetric analysis (TGA) of $(\beta\text{-CD})_2{\cdot}CsI_7{\cdot}13H_2O$.

ter molecules have been removed as evident from the TGA curves. The same curves reveal that the sublimation of iodine starts at $T > 125\,^\circ C$ as was also confirmed by Raman spectra and the variation of conductivity. We used TGA analysis instead of Karl Fischer method, because the presence of iodine in β-Cs does not provide reliable results. Both methods were used in the case of the hydrated β-CD·TERB complex [12].

A pressed pellet of powdered sample, 20 mm in diameter with thickness 1.01 mm, was prepared with a pressure pump (Riken Power model P-1B) at room temperature. Two platinum foil electrodes were pressed at the same time with the sample.

The dielectric measurements were taken in the temperature range of 140–425 K using a low-frequency (0–100 kHz) dynamical signal analyser (DSA-Hewlett–Packard 3561A), which was connected to a personal computer for further processing of the data. A description of the data analysis is given in Ref. [12]. The differential scanning calorimetry (DSC) method (Perkin–Elmer DSC-4 instrument) was used with a thermal analysis data station (TADS) system for the calorimetric measurement.

The Raman spectra were obtained at 4 cm^{-1} resolution from 3500 cm^{-1} to 100 cm^{-1} with data point interval of 1 cm^{-1} using a Perkin–Elmer NIR FT-spectrometer (Spectrum GX II) equipped with an InGaAs detector. The measurements were performed in a temperature range of 30–125 °C (303–398 K). The laser power and spot (Nd: YAG at 1064 nm) were controlled to be constant at 50 mW during the experiments. 500 scans were accumulated.

The experimental X-ray powder diffraction pattern was obtained with a Siemens D 5000 diffractometer (Cu $K\alpha 1 = 1.5406$ Å, Cu $K\alpha 2 = 1.5444$ Å, scan range: 5–55° 2θ, monochromator: graphite crystal, scan speed: 0.045 $2\theta{\cdot}s^{-1}$). The calculation of the theoretical X-ray powder diffraction pattern was performed by the computer program *Powder Cell 2.3* developed by G. Nolze and W. Kraus [13], using the single crystal $(\beta\text{-CD})_2{\cdot}KI_7{\cdot}9H_2O$ diffraction data reported by Saenger in Ref. [2].

3. Results

3.1. Temperature dependence of ε', ε'' and the phase shift ϕ

The temperature dependence of ε' and ε'' over the range 140–300 K at a frequency of 300 Hz is shown in Figs. 3 and 4. The real part ε' increases in a double sigmoid fashion from 4.2 at 140.8 K to 10.2 at 227.5 K and then to 42.6 at 288 K. The inflection point of the first sigmoid is observed at 199.9 K ($\varepsilon' = 6.8$) and that of the second sigmoid at 269.0 K ($\varepsilon' = 29.7$). Above 291 K, ε' increases rapidly to the value $\varepsilon' = 52.5$ at 303.9 K. The $\varepsilon''(T)$ variation presents a double bell-shaped curve with peak values $\varepsilon'' = 1.1$ and $\varepsilon'' = 12.8$ observed at 202.8 K and 274.1 K, respectively. For $T > 282$ K ε'' increases rapidly to the value $\varepsilon'' = 20$ at 291.4 K. By increasing the frequency of the applied field to 1 kHz the two sigmoids in $\varepsilon'(T)$ plot and the two bell-shaped curves in $\varepsilon''(T)$ plot remain separated. For higher applied frequencies (10–100 kHz) the above features become indistinguishable.

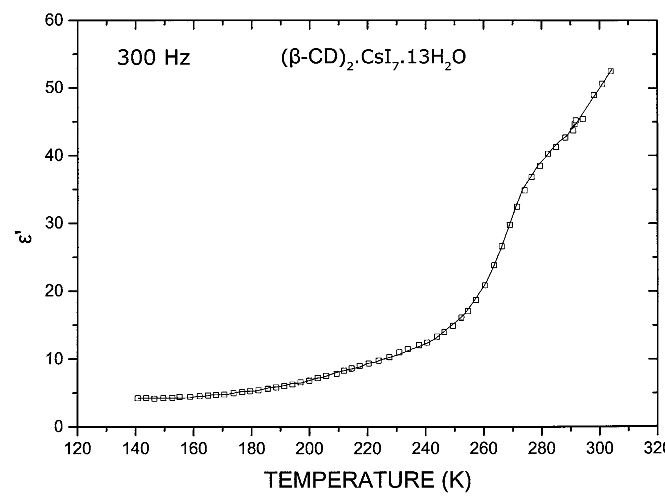

Fig. 3. Temperature dependence of real (ε') part of the dielectric constant of $(\beta\text{-CD})_2{\cdot}CsI_7{\cdot}13H_2O$ at 300 Hz.

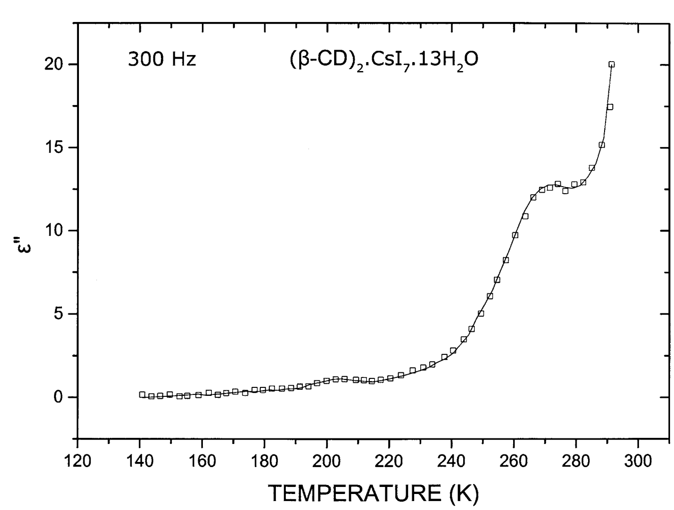

Fig. 4. Temperature dependence of imaginary (ε'') part of the dielectric constant of $(\beta\text{-CD})_2{\cdot}CsI_7{\cdot}13H_2O$ at 300 Hz.

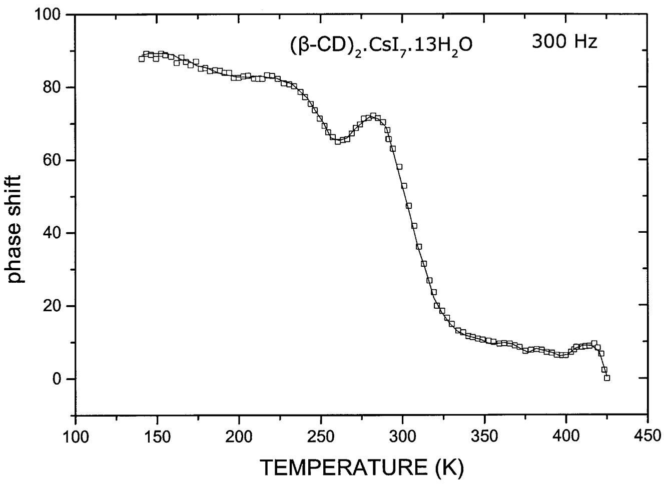

Fig. 5. Temperature dependence of phase shift ϕ of $(\beta\text{-CD})_2\cdot CsI_7\cdot 13H_2O$ at 300 Hz.

The phase shift ϕ at a fixed frequency of 300 Hz (Fig. 5) over the range 140–425 K presents two topical minima 82.5° and 64.9° at 199.9 K and 260.4 K, respectively, followed by an abrupt decrease to a plateau-like region with a third topical minimum 7.5° at 375 K and a fourth topical minimum 6.3° at 397.4 K. Finally at $T > 414.3$ K there is a rapid decrease to the value 0° at 425 K. At higher fixed frequencies all the topical minima are still distinguishable.

3.2. Temperature dependence of conductivity

The temperature variation of the ac-conductivity ($\ln\sigma$ versus $1/T$) under an applied frequency of 300 Hz is shown in Fig. 6 during the heating process. This plot shows two sigmoid curves (a) and (b) in the temperature ranges $4.86\ K^{-1} < 10^3/T < 7.0\ K^{-1}$ and $3.50\ K^{-1} < 10^3/T < 4.86\ K^{-1}$, respectively, and two linear parts (c), (d), in the temperature range $2.66\ K^{-1} < 10^3/T < 3.50\ K^{-1}$. For $10^3/T < 2.66\ K^{-1}$ there are two topical minima at 2.61 and 2.44 K^{-1}. For $10^3/T < 2.44\ K^{-1}$ there

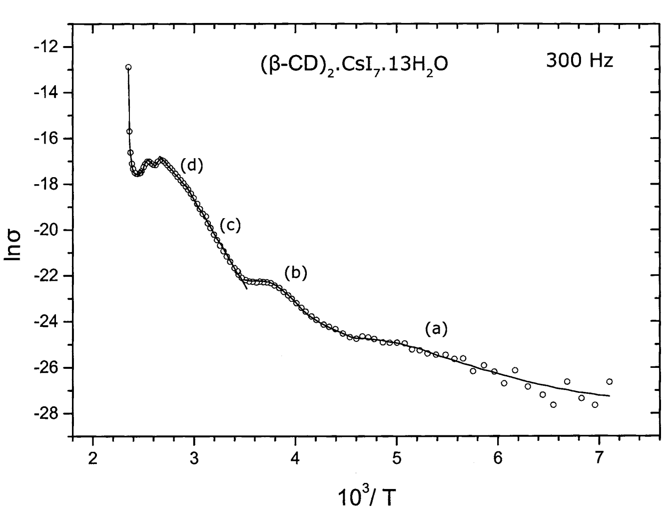

Fig. 6. Temperature dependence of ac-conductivity ($\ln\sigma$ vs $1/T$) for the complex $(\beta\text{-CD})_2\cdot CsI_7\cdot 13H_2O$ at 300 Hz.

is an abrupt increase as a consequence of sublimation of iodine. Thermal hysteresis is totally absent for β-Cs as shown in Fig. 7.

3.3. Calorimetric measurements

The DSC trace of $(\beta\text{-CD})_2\cdot CsI_7\cdot 13H_2O$ recorded with a scan rate of 10 deg min^{-1} shows a small endothermic peak at 80 °C over a temperature range of 35 °C and two strong endothermic peaks with onset temperatures 115 and 135 °C over a temperature range of 25 and 20 °C, respectively, as depicted in Fig. 8.

3.4. Raman spectra

The Raman spectra shown in Figs. 9–11 in the temperature range of 30–125 °C, display an initial peak at 30 °C at 179 cm^{-1} with almost constant intensity as the temperature increases. At 65 °C a shoulder arises at 170 cm^{-1} whose intensity increases with temperature and shifts to the value 166 cm^{-1} in the temperature range of 95–125 °C. The peak intensity

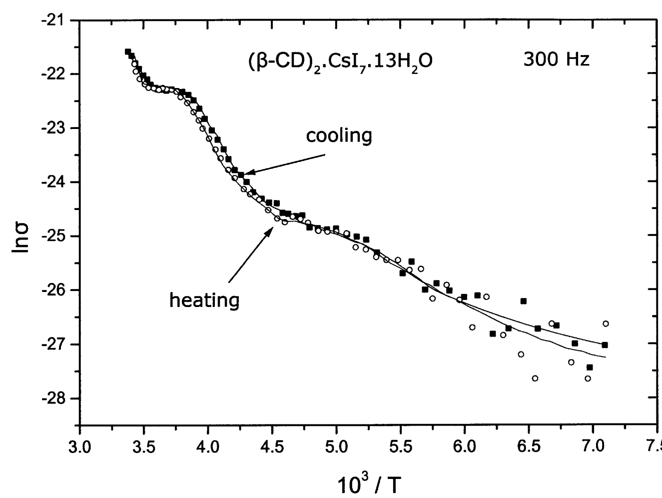

Fig. 7. Temperature dependence of ac-conductivity ($\ln\sigma$ vs $1/T$) for the complex $(\beta\text{-CD})_2\cdot CsI_7\cdot 13H_2O$ during the cooling and heating process, at frequency 300 Hz.

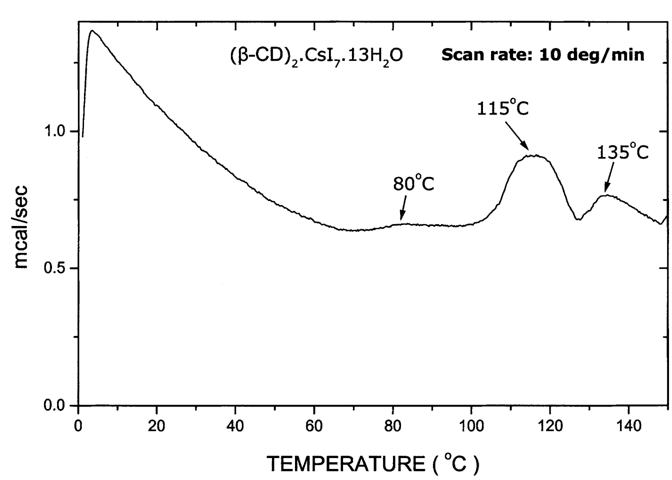

Fig. 8. DSC thermogram of $(\beta\text{-CD})_2\cdot CsI_7\cdot 13H_2O$: heating rate 10 deg min^{-1}.

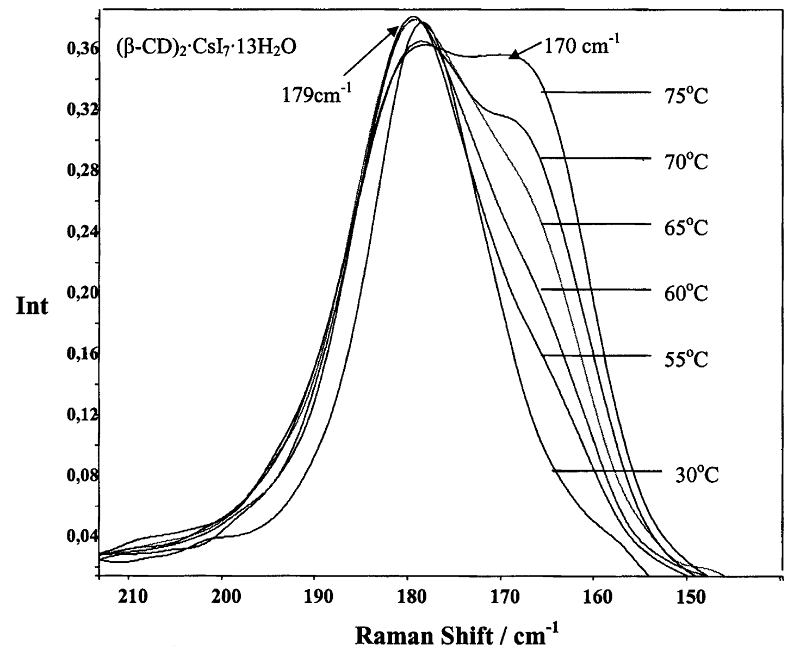

Fig. 9. Raman spectra of (β-CD)$_2$·CsI$_7$·13H$_2$O complex at 30–75 °C.

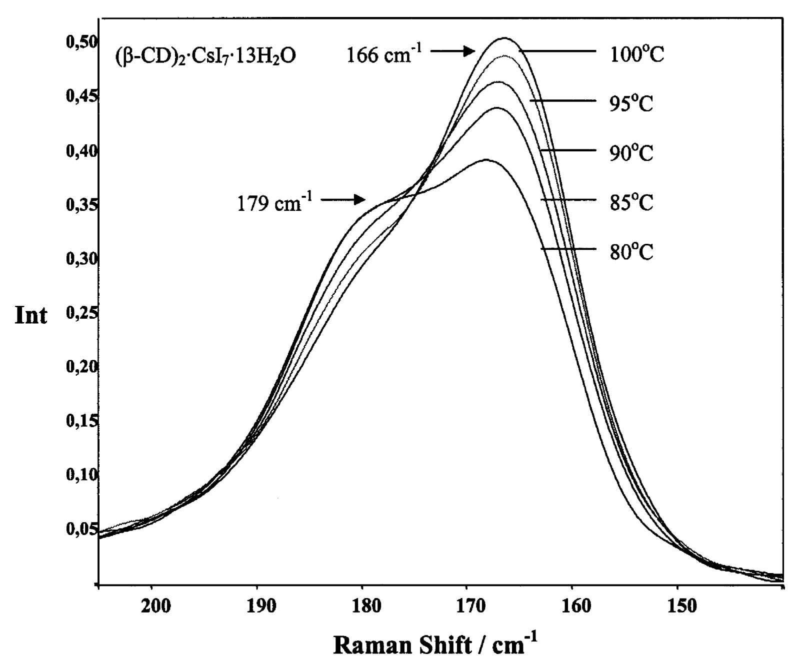

Fig. 10. Raman spectra of (β-CD)$_2$·CsI$_7$·13H$_2$O complex at 80–100 °C.

takes a maximum value 0.53 at 115 °C and then decreases to 0.37 at 125 °C where the initial band at 179 cm^{-1} has disappeared.

3.5. X-ray powder diffraction

Since only the single crystal structure of β-CD complex with potassium metal is available in the literature, we compare in Fig. 12 our experimental X-ray powder diffraction pattern of (β-CD)$_2$·CsI$_7$·13H$_2$O complex with the simulated pattern of (β-CD)$_2$·KI$_7$·9H$_2$O calculated from the single-crystal X-ray diffraction data [2]. It is obvious that β-Cs exhibits an XRD pattern that is in good agreement with that calculated of the β-K complex which is similar to those of β-Ba, β-Cd and β-Li [4,6]. Therefore all these complexes are isomorphous as it was predicted by Saenger [2]. The hump around 25 degrees in (a) is caused by the presence of some amorphous material, while the multitude of peaks at higher 2θ angles is not a result of phase impurities but corresponds to weak Bragg reflections as evident from the calculated pattern (b). Some diffraction peaks exhibit larger relative intensities than those of the theoretical pattern owing to the non-random distribution of crystal orien-

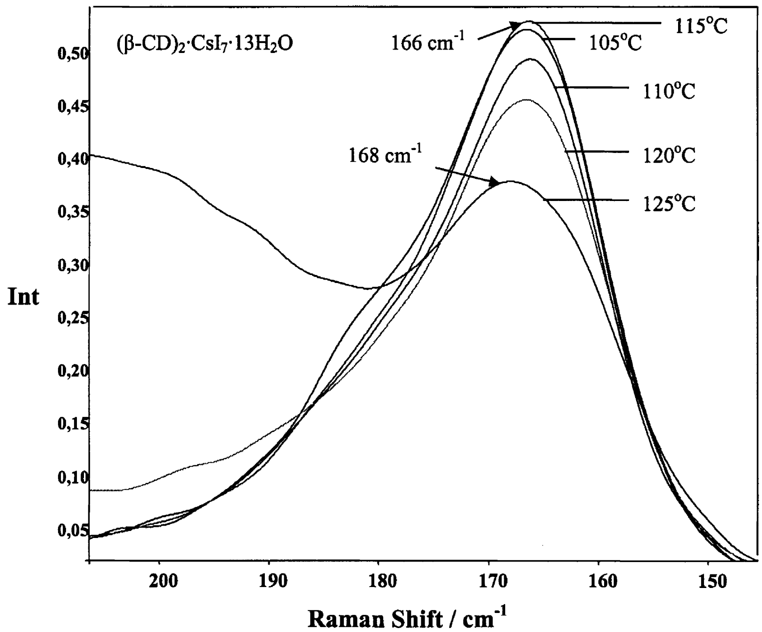

Fig. 11. Raman spectra of (β-CD)$_2$·CsI$_7$·13H$_2$O complex at 105–125 °C.

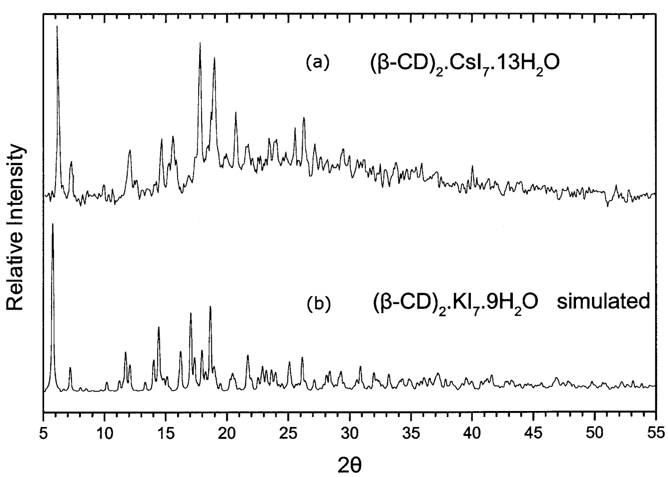

Fig. 12. (a) Experimental X-ray powder diffraction pattern of (β-CD)$_2$·CsI$_7$·13H$_2$O and (b) calculated X-ray powder diffraction pattern from single-crystal data of (β-CD)$_2$·KI$_7$·9H$_2$O complex.

tations (texture). The non-crystalline material does not affect the macroscopic dielectric properties, since the fundamental building blocks (β-CD dimers, coordinated metal ions and heptaiodide units) are expected to be unchanged.

4. Discussion

From the above experimental results, is evident that β-Cs behaves similarly as β-Ba, β-Cd [4] and β-K, β-Li [5,6]. That is, the functions $\varepsilon'(T)$, $\varepsilon''(T)$ and $\phi(T)$ present two sigmoids, two loss peaks and two topical minima, respectively, for $T < 300$ K, indicating that two kinds of water molecules coexist in the crystal lattice, namely tightly bound and easily movable ones. The first $\varepsilon'(T)$ sigmoid, the first $\varepsilon''(T)$ peak and the first $\phi(T)$ minimum correspond to the transformation of some normal hydrogen bonds to those of flip-flop type (order–disorder transition) according to Saenger [7,8]:

$$\mathrm{H_B–O\cdots H_A–O \rightarrow O–H_B\cdots O–H_A}. \tag{2}$$

The transition temperature is found at 199.9 K.

The second sigmoid of $\varepsilon'(T)$, the second peak of $\varepsilon''(T)$ and the second minimum of $\phi(T)$ are clearly distinguished as in the case of β-Ba complex, showing that during the heating process most of the thirteen (13) water molecules per dimer remain tightly bound and only a small number of them are transformed to easily movable ones. This is also confirmed by the DSC trace which shows a small endothermic peak at 80 °C corresponding to the removal of the few easily movable water molecules and a strong peak at 115 °C assigned to the remaining tightly bound water molecules.

The $\ln\sigma$ vs $1/T$ plot reflects all the different effects which take place as the temperature increases. The low temperature sigmoid (a) for $T < 205.7$ K ($10^3/T > 4.86$ K^{-1}) is due to the H$^+$ and OH$^-$ of the normal hydrogen bonds of the water and the β-CD molecules, whereas the high temperature sigmoid (b) for $205.7 \text{ K} < T < 285.7$ K ($3.50 \text{ K}^{-1} < 10^3/T < 4.86 \text{ K}^{-1}$) is caused by the transition of some normal hydrogen bonds to those of flip-flop type and the transformation of few tightly bound water molecules to easily movable ones. The linear part (c) over the range $285.7 \text{ K} < T < 341.2$ K ($2.93 \text{ K}^{-1} < 10^3/T < 3.50 \text{ K}^{-1}$) is due to the contribution of metallic cations which move under the applied alternate field. An activation energy $E_\alpha = 0.64$ eV as calculated from the Arrhenius equation $\sigma = \sigma_0 \exp(-E_\alpha/K_B T)$. In the low temperature range the coordination shell restricts the movement of Cs$^+$ ions, rendering them unable to make an essential contribution to the ac-conductivity. As the temperature increases the tetrahedral arrangement is broken, resulting in the release of positive ions which are free to oscillate back and forth with the frequency of the field and to contribute to the total ac-conductivity. During this process there is a gradual transformation of the tightly bound water molecules to easily movable ones, giving rise to proton diffusion via a Grotthuss mechanism [9,10]. For this reason the phase shift in Fig. 5 drops rapidly for $T > 282.2$ K.

The linear part (d) in the temperature range of 68–102 °C ($2.66\ \mathrm{K}^{-1} < 10^3/T < 2.93\ \mathrm{K}^{-1}$) with activation energy $E_\alpha = 0.45$ eV shows a lower increase of the ac-conductivity because the concentration of charge carriers ($H_2O_{\mathrm{easilymovable}}$) is reduced due to their gradual escape from the sample (DSC trace in Fig. 8). At higher temperatures the conductivity does not follow the Arrhenius exponential behaviour but decreases to a topical minimum at 109 °C ($10^3/T = 2.61\ \mathrm{K}^{-1}$) due to the removal of all easily movable water molecules. The new increment up to 122 °C ($10^3/T = 2.53\ \mathrm{K}^{-1}$) corresponds to the transformation of the remaining tightly bound water molecules according to Eq. (1). Finally the conductivity decreases up to 136.8 °C ($10^3/T = 2.44\ \mathrm{K}^{-1}$) due to the removal of all the water molecules. This explanation is in agreement with the presence of the endothermic peak at 115 °C in the DSC trace. The rapid increase of the ac-conductivity for $10^3/T < 2.44\ \mathrm{K}^{-1}$ is due to the sublimation of iodine (third endothermic peak at 135 °C in Fig. 8). This effect shows that the polyiodide chains contribute efficiently to the conductivity for $T > 130$ °C. At lower temperatures their contribution is negligible, as evident from the spectroscopic results.

The Raman peaks at 179, 170 and 166 cm^{-1} correspond to d(I–I) bond distances 2.72, 2.75 and 2.77, respectively, according to a linear correlation of Raman frequencies υ(I–I) versus the d(I–I) [14]. So the initial band at 179 cm^{-1} could be assigned to an average d(I–I) distance of 2.72 Å, resulting from the simultaneous major and minor occupancies of the I_2 units, while the peak at 166 cm^{-1} corresponds to the separation distance of the two disordered atoms I(4A)–I(5A) = 2.77 Å. The peak at 170 cm^{-1} corresponding to d(I–I) = 2.75 Å is attributed to an intermediate state in which a charge transfer interaction $I_2 \cdots I^-{}_3 \rightarrow I^-{}_3 \cdots I_2$ takes place due to the symmetric stretch of iodine molecules [15]. Thus, during the heating process a lengthening of I(4B)–I(5B) distances of I_2 units to 2.77 Å takes place. It has been shown that the symmetric $I^-{}_3$ ion with I–I distance 2.90 Åhas a Raman peak at 110 cm^{-1} [3]. In our case the interiodine distance I(1)–I(2) = 3.003 Å of the $I^-{}_3$ units indicates that the corresponding Raman peak is located at frequencies below 100 cm^{-1} which was not possible to detect. All the above results show that the electronic density remains localized since there is no interaction between the neighbouring $I^-{}_7$ units (I(5)–I(5) = 4.50 Å) until the sublimation of iodine starts. This process shortens the distances between the heptaiodide ions, providing conducting paths for the localized charges [16].

5. Conclusions

The temperature dependences of ε', ε'' and the phase shift ϕ of the $(\beta\text{-CD})_2\cdot CsI_7\cdot 13H_2O$ complex for $T < 300$ K, reveal the existence of two kinds of water molecules, tightly bound and easily movable ones. The transition of normal hydrogen bonds to those of flip-flop type happens at 199.9 K. As the temperature increases most of the thirteen water molecules per dimer remain tightly bound and only a small percentage of them become easily movable. The small endothermic peak of the DSC trace, with onset temperature 80 °C, is related to the easily movable water molecules while the strong peaks at 115 and 135 °C are caused by the tightly bound water molecules and the sublimation of iodine, respectively.

The different components contributing to the conductivity are detected from the $\ln\sigma$ vs $1/T$ plot, indicated by the sigmoids (a), (b) and the linear parts (c) and (d). The low temperature sigmoid (a), for $T < 205.7$ K is due to the H^+ and OH^- of the normal hydrogen bonds of the water and the β-CD molecules, whereas the high temperature sigmoid (b) for $205.7\ \mathrm{K} < T < 285.7$ K is caused by the transition of some normal hydrogen bonds to those of flip-flop type and the transformation of few tightly bound water molecules to easily movable ones. The linear parts (c), (d) over the range $285.7\ \mathrm{K} < T < 375.9$ K with activation energies 0.64 and 0.45 eV, respectively, are related to the contribution of the metal ions and the removal of the water molecules to the ac-conductivity.

The Raman peaks at 179, 170 and 166 cm^{-1} indicate charge transfer interactions in the $I^-{}_7$ units. Their negative charge remains localized with negligible contribution to the conductivity until the sublimation of iodine starts.

Acknowledgements

This work was partly supported by Grant No. 70/4/3347SARG, NKUA. We thank prof. K. Viras for his assistance in the Raman Spectra and DSC thermograms.

References

[1] M. Noltmeyer, W. Saenger, J. Am. Chem. Soc. 102 (1980) 2710–2722.
[2] C. Betzel, B. Hingerty, M. Noltmeyer, G. Weber, W. Saenger, J. Incl. Phenom. 1 (1983) 181–191.
[3] E.M. Nour, L.H. Chen, J. Laane, J. Phys. Chem. 90 (1986) 2841–2846.
[4] V.G. Charalampopoulos, J.C. Papaioannou, Molec. Phys. 103 (2005) 2621–2631.
[5] J.C. Papaioannou, Molec. Phys. 102 (2004) 95–99.
[6] J.C. Papaioannou, V.G. Charalampopoulos, P. Xynogalas, K. Viras, in preparation.
[7] C. Betzel, W. Saenger, B.E. Hingerty, G.M. Brown, J. Am. Chem. Soc. 106 (1984) 7545–7557.
[8] V. Zabel, W. Saenger, S.A. Mason, J. Am. Chem. Soc. 108 (1986) 3664–3673.
[9] N. Agmon, Chem. Phys. Lett. 244 (1995) 456–462.
[10] B.V. Merinov, Solid State Ionics 84 (1996) 89–96.
[11] P. Svensson, L. Kloo, Chem. Rev. 103 (2002) 1649–1684.
[12] J.C. Papaioannou, N. Papadimitropoulos, I. Mavridis, Molec. Phys. 97 (1999) 611–627.
[13] G. Nolze, W. Kraus, Powder Diffr. 13 (1998) 256–259.
[14] F. Demartin, P. Deplano, F.A. Devillanova, F. Isaia, V. Lippolis, G. Verani, Inorg. Chem. 32 (1993) 3694–3699.
[15] P. Svensson, L. Kloo, J. Chem. Soc. Dalton Trans. (2000) 2449–2455.
[16] A. Oza, Cryst. Res. Technol. 19 (1984) 697–707.